Macromolecules **2003,** *36,* 8695−8703

Chlorinated Guest Orientation and Mobility in Clathrate Structures Formed with Syndiotactic Polystyrene

Alexandra R. Albunia,*,† Sergio Di Masi,† Paola Rizzo,† Giuseppe Milano,† Pellegrino Musto,‡ and Gaetano Guerra†

Dipartimento di Chimica, Università degli Studi di Salerno, via S.Allende, 84081 Baronissi (SA), Italy, and Institute of Chemistry and Technology of Polymers, National Research Council of Italy, via Campi Flegrei 34, 80078 Pozzuoli (Na), Italy

Received July 9, 2003; Revised Manuscript Received September 3, 2003

ABSTRACT: Syndiotactic polystyrene films uniaxially stretched at different draw ratios, and including different crystalline (δ and γ) phases as well as clathrate phases with 1,2-dichloropropane, 1,2-dichloroethane, and 1-chloropropane, have been studied by combined infrared linear dichroism and X-ray diffraction measurements. Information relative to the orientation and mobility of trans and gauche conformers of these chlorinated guests in their clathrate structures with syndiotactic polystyrene has been achieved by comparison between experimentally evaluated and calculated vibrational transition moment directions of conformationally sensitive infrared peaks of the guest molecules.

Introduction

Syndiotactic polystyrene (s-PS), whose synthesis was reported several years ago,[1,2] has a very high melting point (close to 270 °C), high crystallization rate, high chemical stability, and excellent workability in most thermoplastic fabrication technologies. It is characterized by a complex polymorphic behavior, which, making some simplifications, can be described in terms of two crystalline forms, α and β, containing planar zigzag chains and two forms, γ and δ, containing $\mathbf{s}(2/1)2$ helical chains.[3] These helical chains also characterize several clathrate structures, for which the intensity and locations of the crystalline reflections in the X-ray diffraction patterns slightly change with the kind and amount of the included guest molecules.[3−6]

Sorption studies from liquid and gas phases, into s-PS samples being in the nanoporous δ form,[7] have shown that this thermoplastic material is able to absorb selectively some volatile organic compounds (mainly alogenated or aromatic hydrocarbons) also when present at low concentrations,[8−11] forming the corresponding clathrate forms. These sorption studies have suggested that this material is promising for applications in chemical separations as well as in water and air purification. In particular, thin polymeric films have been suggested as sensing elements of molecular sensors.[12]

FTIR studies on clathrate samples, including chlorinated hydrocarbon guests, have shown that the trans conformation of 1,2-dichloroethane (DCE) and 1,2-dichloropropane (DCP) is largely prevailing in the clathrate phase, while the trans and gauche conformations are nearly equally populated when both chlorinated compounds are sorbed in the amorphous phase. Completely different is the 1-chloropropane (CP) behavior, for which the population of the conformers remains essentially unaltered as a consequence of clathration into s-PS.[10,11,13]

As for the clathrate with DCE, structural studies, based on X-ray diffraction on fibers[6] associated with molecular mechanics calculations,[11] have allowed the establishment of the low-energy locations of the DCE trans conformer into the clathrate unit cell. As for the clathrates with DCP and CP, structural studies based on X-ray diffraction of fibers are not available. Such studies would be less informative due to the structural disorder associated with the lower molecular symmetry as well as with the presence of two enantiomers (R and S) for DCP and two conformers (trans and gauche) for CP. Molecular mechanics studies suggested possible minimum-energy locations in the clathrate phases for both DCP and CP conformers and rationalized the conformational equilibria of these chlorinated compounds upon clathration.[11]

In this paper, syndiotactic polystyrene films uniaxially stretched at different draw ratios, and including different crystalline (δ and γ) and clathrate phases (with DCP, DCE, and CP), have been studied by combined infrared linear dichroism measurements and X-ray diffraction evaluations of polymer chain axis orientation factors relative to the crystalline phase.

Moreover, by following a procedure analogous to that one generally used to evaluate transition moment directions for polymeric vibrational modes,[14] transition moment directions of guest vibrational modes with respect to the crystalline polymer chain axis have been evaluated. These experimentally evaluated transition moment vector directions have been compared with those obtained by density functional theory (DFT) calculations for isolated molecules, by assuming guest locations in the crystalline host cavity as obtained by the above-cited X-ray diffraction structural studies,[6] and/or by molecular mechanics calculations.[11]

Experimental Section

Materials. Syndiotactic polystyrene was supplied by Dow Chemical under the trademark Questra 101. ^{13}C nuclear magnetic resonance characterization showed that the content of syndiotactic polystyrene triads was over 98%. The weight-average molar mass obtained by gel permeation chromatography (GPC) in trichlorobenzene at 135 °C was found to be $M_w = 3.2 \times 10^5$ with the polydispersity index $M_w/M_n = 3.9$.

---

* Corresponding author: e-mail aalbunia@unisa.it.

† Università degli Studi di Salerno.

‡ National Research Council of Italy.

10.1021/ma034964x CCC: $25.00

s-PS amorphous films, 100−120 μm thick, were obtained by extrusion of the melt with an extrusion head of 200 mm × 0.5 mm.

Oriented films were obtained by monoaxial stretching of the extruded ones, at different draw ratios up to $\lambda = 3.8$ at constant deformation rate of 0.1 s^{-1}, in the temperature range 105−110 °C with a Brukner stretching machine. The stretched films are still essentially amorphous and have been crystallized into the nanoporous δ form by exposure for 3 days to CS_2 vapors, followed by treatment under vacuum at 40 °C for other 3 days. The orientation of the crystalline phase is characterized by a high degree of parallelism of the chain axes with respect to the stretching direction (f_c up to 0.95) and a low degree of parallelism of the *ac* planes with respect to the film plane (f_{010} up to 0.3).[15]

The clathrate films were obtained from δ form films by exposure for 30 min to DCE vapors or by immersion for 16 h in CP and DCP. A partial desorption of the chlorinated molecules was allowed in order to get their substantial removal from the amorphous phase. The content of chlorinated molecules in the films was determined by thermogravimetric measurements (TGA). At room temperature, the clathrates with DCP are stable for years while the clathrates with the more volatile DCE and CP guests lose the guest molecules, giving back the nanoporous δ phase, after several months and few hours of desorption, respectively.

Methods. *X-ray Diffraction.* The degree of axial orientation relative to the crystalline phase has been formalized on a quantitative numerical basis using Hermans' orientation function:[14a,b]

$$f_{c,RX} = (3\overline{\cos^2 x} - 1)/2 \tag{1}$$

by assuming $\overline{\cos^2 x}$ as the squared average cosine value of the angle, *x*, between the draw direction and the crystallographic *c* (chain) axis. The orientation factor, f_c, is equal to 1 for perfect alignment ($x = 0°$), whereas it is equal to −0.5 for perpendicular alignment ($x = 90°$). For random orientation $\overline{\cos^2 x}$ is $^1/_3$, and hence f_c is zero.

Since for nanoporous δ and for clathrate phases an intense (*002*) reflection is present, the quantity $\overline{\cos^2 x}$, and hence the degree of axial orientation $f_{c,RX}$, can be easily experimentally evaluated by

$$\overline{\cos^2 x} = \overline{\cos^2 \chi_{002}} = \frac{\int_0^{\pi/2} I(\chi_{002}) \cos^2 \chi_{002} \sin \chi_{002}\, d\chi_{002}}{\int_0^{\pi/2} I(\chi_{002}) \sin \chi_{002}\, d\chi_{002}} \tag{2}$$

where $I(\chi_{002})$ is the intensity distribution of the 002 diffractions on the Debye rings and χ_{002} is the azimuthal angle measured from the meridian.

The diffracted intensities $I(\chi_{002})$ were obtained by using an AFC7S Rigaku automatic diffractometer (with monochromatic Cu Kα radiation) and were collected sending the X-ray beam parallel to the film surface and perpendicular to the stretching direction.

Infrared Spectroscopy. Infrared spectra were obtained at a resolution of 2.0 cm^{-1} with a Vector 22 Bruker spectrometer equipped with deuterated triglycine sulfate (DTGS) detector and a Ge/KBr beam splitter. The frequency scale was internally calibrated to 0.01 cm^{-1} using a He−Ne laser. A total of 32 scans were signal-averaged to reduce the noise. Polarized infrared spectra were recorded by use of a SPECAC 12000 wire grid polarizer.

As far as infrared spectroscopy is concerned, the axial orientation function is given by[14c,d]

$$f_{c,IR} = \frac{R-1}{R+2}\,\frac{2\cot^2\alpha + 2}{2\cot^2\alpha - 1} \tag{3}$$

where $R = A_{\parallel}/A_{\perp}$ is the dichroic ratio, $A_{\parallel}$ and $A_{\perp}$ being the measured absorbance for electric vectors parallel and perpendicular to the draw direction, respectively, and α is the angle between the chain axis and the transition moment vector of the vibrational mode.

As usual, an order parameter *S* can be defined as the ratio

$$S = (R - 1)/(R + 2) \tag{4}$$

The angle α can be determined from theory, and dichroic measurements allow the calculation of the orientation factor. Moreover, the α angle can be determined by comparison with an independent technique (X-ray diffraction, birefringence). In the present paper, as discussed later in detail, the α angles relative to both host and guest vibrational modes have been evaluated by assuming the orientation function of the crystalline phase, as evaluated by X-ray diffraction measurements, by using eqs 1 and 2.

Computational Methods. Vibrational frequencies calculations have been performed by density functional theory (DFT) method after geometry optimization at the B3LYP/6-31G** level. The transition moment direction for the *i*-normal mode has been obtained from electric dipole moment (μ) derivatives $\partial\mu/\partial Q_i$ (indicated as $\mu_1^{(i)}$ in Figure 10) with respect to the corresponding *i*-normal coordinate (Q_i).[16] Details about molecular mechanics procedures for the considered host−guest systems and force field are reported in ref 11. All quantum mechanical calculations have been performed by the Gaussian98 program.[17]

Results and Discussion

Infrared Dichroism of Host and Guest Molecules. FTIR spectra in the wavenumber range 1400−450 cm^{-1} of uniaxially oriented s-PS films ($\lambda \approx 3$), taken with polarization plane parallel and perpendicular to the draw direction, are shown in Figure 1 by thin and thick lines, respectively. The spectrum of the semicrystalline sample including the nanoporous crystalline δ phase (Figure 1A) clearly indicates the presence of several peaks that are highly dichroic. In particular, high dichroic ratios are measured for the peaks at 505($\perp$), 548($\perp$), 571($\parallel$), 769($\parallel$), 934($\perp$), 943($\parallel$), 1278($\parallel$), 1320($\perp$), and 1354($\parallel$) cm^{-1}, all corresponding to vibrational modes of the crystalline s(2/1)2 helices,[18] which are labeled "c" in Figure 1A. A dichroic ratio not far from 1 is instead observed for the peaks at 840 and 1154 cm^{-1}, possibly due to a prevailing contribution of the amorphous phase (labeled "a" in Figure 1A). These observations clearly indicate that, as usually occurs for semicrystalline polymers, high degrees of orientation are achieved more readily by the crystalline phase, while the amorphous phase gets substantial orientation only for extreme drawing conditions.

The order parameters for the host helical peaks at 571 and 1320 cm^{-1} are reported in Figure 2 versus the draw ratio (curves A and B, respectively). It is clearly apparent that, for both peaks, the order parameter is negligible at least up to $\lambda = 1.5$, while their limiting values ($S = 1$ or $S = -0.5$, corresponding to $f_{c,IR} = 1$ for α equal to 0° and 90°, respectively) are nearly reached already for $\lambda = 2.5$. The observation of *S* values close to the limiting ones indicates that the α angles relative to the 571 and 1320 cm^{-1} peaks are close to 0° and 90°, respectively. These results suggest that the order parameter of the 571 cm^{-1} peak (curve A of Figure 2) can be directly used as a measure of the axial orientation function ($f_{c,IR}$). This will be later confirmed by the comparison of these order parameters with the orientation function data, as taken by X-ray diffraction measurements (next two sections).

The FTIR spectra of oriented nanoporous s-PS films, like that one of Figure 1A, remain substantially unal-

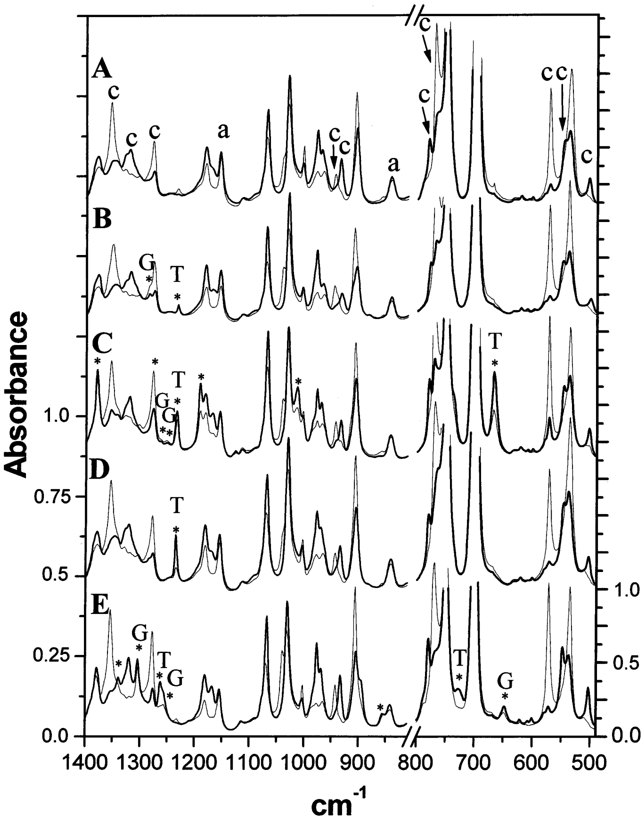

Figure 1. FTIR spectra for the wavenumber range 1400−450 cm^{-1}, taken with polarization plane parallel (thin lines) and perpendicular (thick lines) to the draw direction, for uniaxially oriented s-PS films (for $\lambda \approx 3$) including different crystalline and clathrate phases: (A) nanoporous crystalline δ phase; (B) γ phase with 4.3% of DCE in the amorphous phase; (C) clathrate with DCP; (D) clathrate with DCE; (E) clathrate with CP.

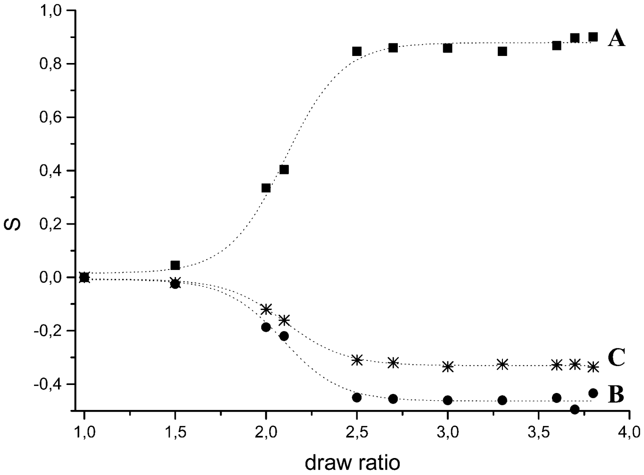

Figure 2. Order parameter $S = (R - 1)/(R + 2)$ vs the film draw ratio, as obtained by the infrared dichroic ratios, of two host helical peaks at 571 (A) and 1320 cm^{-1} (B) and of the DCE guest peak at 1234 cm^{-1} (C).

tered as a consequence of annealing at 160 °C under tension, leading to a transition between the two helical crystalline forms, i.e., from the nanoporous δ form toward the more dense γ form.[3,18]

The FTIR spectrum of an oriented γ form s-PS film, after absorption of 4.3 wt % of DCE, which as usual is only included into the amorphous phase,[10] is shown in Figure 1B. The relative intensities of the peaks at 1234 and 1285 cm^{-1} indicate the presence of both trans and gauche conformers in a ratio close to 0.32, not far from the value observed for liquid DCE (0.35).[19] Moreover, the substantial absence of dichroism for these peaks clearly indicates the nearly negligible orientation for the chlorinated molecules included into the amorphous phase.

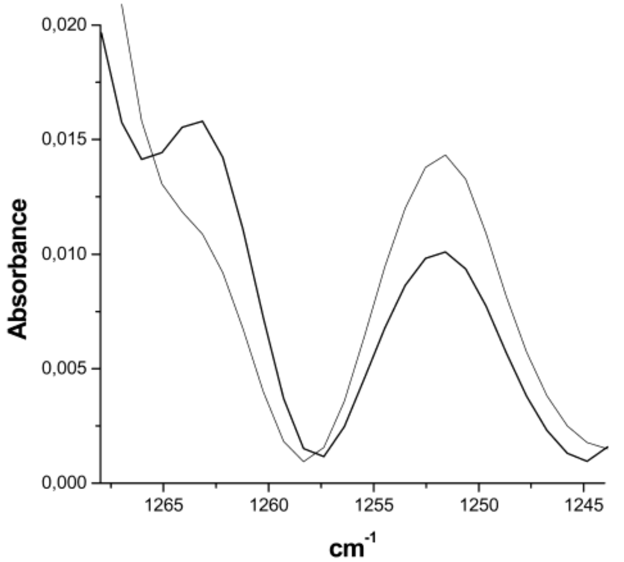

Figure 3. FTIR spectrum for the wavenumber range 1270−1240 cm^{-1}, taken with polarization plane parallel (thin lines) and perpendicular (thick lines) to the draw direction, for an uniaxially oriented film ($\lambda \approx 3$) including the s-PS/DCP clathrate phase.

FTIR spectra of oriented nanoporous δ form s-PS films, after sorption and partial desorption of DCP (9.8 wt %), DCE (6 wt %), and CP (9.5 wt %), are shown in parts C, D, and E, respectively, of Figure 1. First of all, it is worth noting that the dichroism of the polymer host peaks remains essentially unaltered as a consequence of guest absorption, although the clathration has been achieved for CP and DCP by immersion in liquid solvents for prolonged periods. The well-resolved conformationally sensitive peaks of the chlorinated guests,[19−21] which are indicated by asterisks in Figure 1C−E, are generally highly dichroic. Also, the weak DCP peaks, in the 1270−1240 cm^{-1} range, due to the minor amount of G conformer (Figure 1C), which are better shown by the enlarged spectrum of Figure 3 are highly dichroic. These high dichroic ratios (Figures 1C−E and 3) clearly indicate that all the considered guest molecules when included into the clathrate phase, independently of their conformation, present some degree of order with respect to the draw direction.

Since the molecules absorbed in the amorphous phase are substantially unoriented (Figure 1B), the measured dichroic ratios strongly depend on the possible presence of chlorinated molecules into that phase. As discussed in detail in previous papers,[10,13] after sorption into semicrystalline nanoporous samples, guest molecules can be partitioned almost evenly in amorphous and clathrate phases, but the amorphous phase loses the chlorinated molecules at a much faster rate than does the clathrate one, and after substantial desorption, most of the residual low molecular weight molecules are located in the crystalline phase. As a consequence, the order parameters of the guest peaks tend to increase (in absolute value) with guest desorption, gradually reaching a plateau value. This is shown, for instance, in Figure 4 for the order parameter S relative to a T

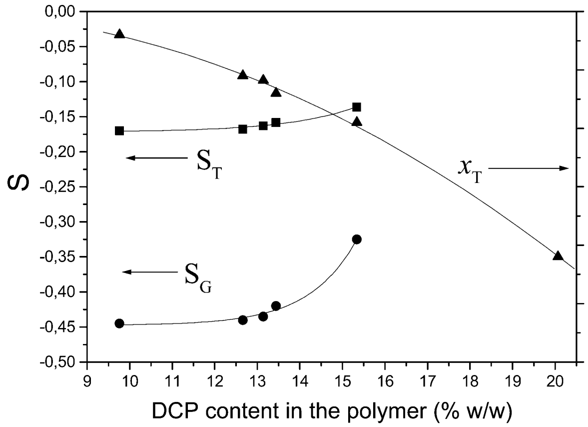

Figure 4. Order parameters S_T and S_G relative to a T (1234 cm^{-1}) and a G (1263 cm^{-1}) peak of DCP (left scale), and fraction of DCP molecules in the trans conformation (x_T), evaluated by the relative intensities of the 1234 and 1263 cm^{-1} peaks as described in ref 13b (right scale) reported vs the DCP weight content in the film. The data have been collected for a δ form s-PS films stretched at $\lambda \approx 3$, after absorption of liquid DCP and its progressive partial desorption at room temperature.

(1234 cm^{-1}) and a G (1263 cm^{-1}) peak of DCP absorbed into δ form s-PS films, which is reported versus the DCP content in the film (corresponding to different desorption times at room temperature).

In the same plot of Figure 4, the fraction of DCP molecules in the trans conformation (x_T), evaluated by the relative intensities of the 1234 and 1263 cm^{-1} peaks as described in ref 13b, is also reported. It is apparent that both order parameters reach nearly constant values for DCP content lower than 10 wt %, and correspondingly the fraction of trans conformer approaches unity.[13b] This clearly confirms that the plateau values reached for the order parameters, by decreasing the guest content, can be considered as those of the guest molecules in the clathrate phases.

It is also worth noting that by assuming a crystallinity of 35%, as evaluated by the intensity of the helical FTIR peaks,[22] since the stoichiometric value of the clathrate phase is 4 monomer units per 1 guest molecule,[6] a completely filled clathrate phase and a completely desorbed amorphous phase would correspond to a DCP content not far from 9 wt %.

The samples considered in the following quantitative analyses have been partially desorbed at room temperature, so that they contain only minor amounts of chlorinated molecules in the amorphous phase and hence correspond or are close to plateau values of dichroic ratios.

As for DCP clathrate spectra (Figure 1C), although the trans conformer largely prevails in the clathrate structure, it is possible to study also some weak peaks relative to the guest gauche conformer since they are located in a wavenumber range where polymer peaks are not present (Figure 3). In fact, quantitative evaluations can be afforded not only for two T peaks but also for the weak G peaks at 1263 and 1254 cm^{-1}.

As for DCE clathrate spectra (Figure 1D), only the 1234 cm^{-1} peak is easily available to quantitative evaluations. In fact, since most of the guest molecules are in the trans conformation,[10,13] the G peaks are too weak. Moreover, for the other T peaks there is an unfavorable superposition with some polymer peaks.

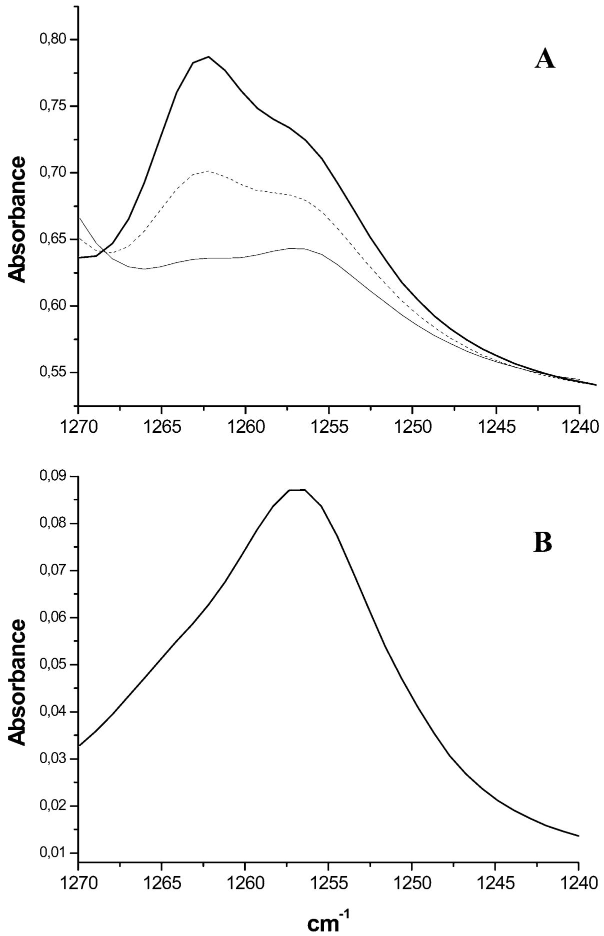

Figure 5. FTIR spectra for the wavenumber range 1270−1240 cm^{-1}: (A) taken with polarization plane parallel (thin lines) and perpendicular (thick lines) to the draw direction, for an uniaxially oriented film ($\lambda \approx 3$) including the s-PS/CP clathrate phase; (B) for liquid CP.

As for CP clathrates, for which substantial amounts of both trans and gauche conformers are included into the clathrate phase, few T and G peaks are available for quantitative evaluations (Figure 1E). In particular, in the 1270−1240 cm^{-1} range, two dichroic peaks, the more intense being located at 1263 cm^{-1} and the weaker at 1257 cm^{-1}, are clearly apparent (Figures 1E and 5A). It is worth noting that liquid CP (as well as CP absorbed into the amorphous s-PS phase) correspondingly shows only a shoulder at 1263 cm^{-1} and an intense peak at 1257 cm^{-1} (Figure 5B). This clearly indicates that the intensity of the 1263 cm^{-1} is strongly increased by inclusion of the CP guest molecule into the s-PS host crystalline phase.

For all these conformationally sensitive guest peaks the dichroic ratio and the order parameter S have been evaluated as a function of the draw ratio of the nanoporous s-PS film. Just as an example, the order parameter of the peak at 1234 cm^{-1} relative to the trans conformer of DCE is reported in Figure 2 (curve C) vs the film draw ratio.

Host Crystalline Phase Orientation by X-ray Diffraction. Photographic X-ray diffraction patterns collected with the X-ray beam perpendicular and parallel to the film plane (not shown) indicate that essentially only an axial orientation, which is a preferential orientation of the chain axes parallel to the draw direction, is present.

The crystalline phase orientation has been evaluated by azimuthal scans relative to the (002) reflection, for

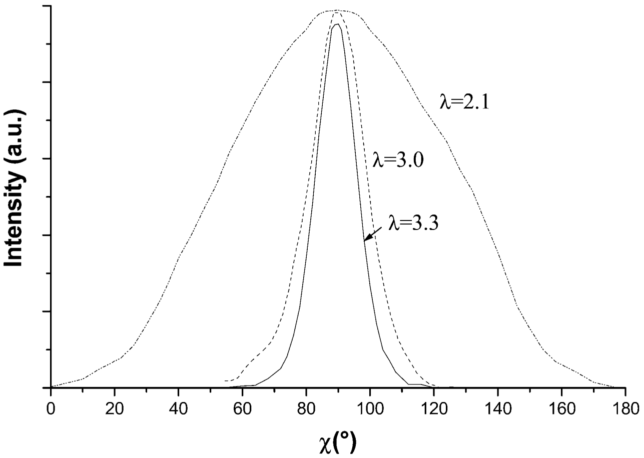

Figure 6. Azimuthal scans at $2\theta_{\mathrm{Cu\ K}\alpha} \approx 23°$, relative to the (002) reflection of the s-PS/DCE clathrate form, for film samples stretched at three different draw ratios.

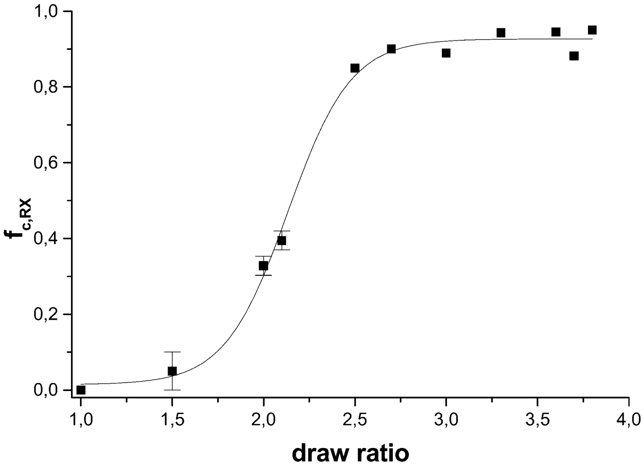

Figure 7. Orientation factor of the crystalline phase, $f_{c,RX}$, as evaluated by eqs 1 and 2 on the basis of azimuthal scans like those of Figure 6, reported versus the film draw ratio.

the sPS films stretched at different draw ratios, which include the nanoporous δ phase or the DCE clathrate phase.

Just as an example, azimuthal scans relative to the (002) reflection of the sPS/DCE clathrate form (at $2\theta_{\mathrm{Cu\ K}\alpha} \approx 23°$), for samples stretched at three different draw ratios, are shown in Figure 6. The orientation factors of the crystalline phase, $f_{c,RX}$, as evaluated by eqs 1 and 2 on the basis of azimuthal scans like those of Figure 6, are reported versus the draw ratio in Figure 7 for DCE clathrate films. It is apparent that the crystalline orientation function is close to the maximum value (unity) for films drawn at draw ratios higher than 2.5, while the orientation function is substantially negligible for draw ratios lower than 1.5.

Host Crystalline Phase Orientation by Infrared Dichroism. The orientation factors of the conformationally ordered chains (included in the crystalline phase) can be evaluated by FTIR measurements on the basis of eq 3 if the α angle between the transition moment vector relative to the peak of interest and the chain axis is known.

The α angles between the crystalline *c* axis and the transition moment vectors for the s-PS peaks, corresponding to long helical sequences (571 and 1320 cm^{-1}), have been evaluated by using eq 3 and by assuming the orientation factor as evaluated by X-ray diffraction measurements of the previous section.

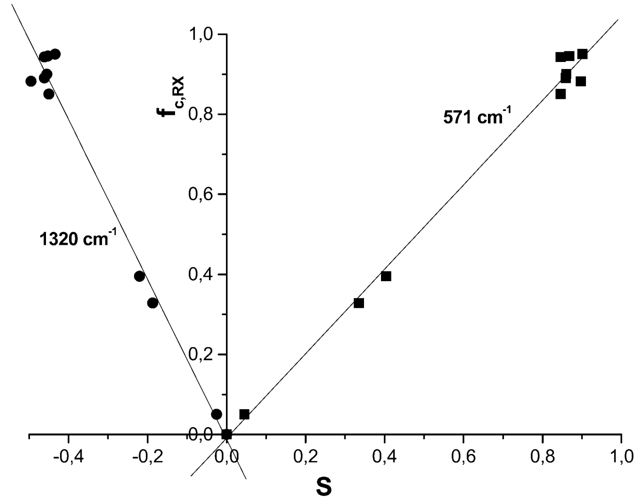

Figure 8. Crystalline phase orientation factors of DCE clathrate films stretched at different draw ratios, as evaluated by X-ray diffraction ($f_{c,RX}$) vs the order parameter *S*, as obtained by dichroic ratios of the 571 and 1320 cm^{-1} host helical peaks. The slopes of the two straight lines allow to evaluate the α angles between the crystallographic *c* axis and the dipole moment vector of the vibrational modes.

In particular, for DCE clathrate films stretched at different draw ratios, by reporting the crystalline phase orientation factors, as evaluated by X-ray diffraction ($f_{c,RX}$) vs the order parameter *S* obtained by dichroic ratios of the 571 and 1320 cm^{-1} helical peaks (Figure 8), straight lines with slopes close to 1 and −2 and as a consequence α values close to 0° and 90° have been obtained, respectively.

Of course, the knowledge of these α values allows an easy evaluation of the crystalline phase orientation for any helical s-PS sample, just based on a dichroic ratio measurement for one of these two peaks. In particular, since the transition moment vector for the peak at 571 cm^{-1} is parallel to the chain axis, the corresponding orientation function is directly equal to the order parameter *S* (like, for instance, that one shown by curve A of Figure 2).

Transition Moment Vector Directions of Guest Vibrational Modes. *Experimental Evaluation of Transition Moment Directions of Guest Vibrational Modes with Respect to the Chain Axis of the Host Crystalline Phase.* In this section, a quantitative comparison between dichroic ratios of polymer host helical peaks and of guest peaks, by using a procedure analogous to one described in the previous section, is presented. The infrared order parameters *S*, as evaluated by dichroic ratios of the conformationally sensitive peaks of the three chlorinated guests, labeled as T or G in the spectra of Figure 1C−E, for the guests DCP, DCE, and CP, are reported in Figure 9A−C, respectively. In particular, the order parameters are plotted versus the orientation factors relative to the helical chains of the clathrate phases, as evaluated by the dichroic ratio of the 571 cm^{-1} infrared peak ($f_{c,IR}$).

In this respect, it is worth noting that the dichroism of the peaks of the helical (crystalline) polymer host is affected by the orientation distribution of the crystallites with respect to the draw direction, while the dichroism of the peaks of a guest molecule can be also affected by its mobility into the crystalline cavity.

By applying eq 3 to the data of Figure 9, the α values listed in the eighth column of Table 1 for different guest

Table 1. Conformationally Sensitive Peaks of Gauche (G) and Trans (T) Conformers of the Three Chlorinated Guest Molecules, for Which the Dichroism Analysis Has Been Affected[a]

guest	peak (cm^{-1})	gas phase (cm^{-1})	calcd (cm^{-1})	conformer	mode	ϕ (deg)	α (deg)	α_{calc} (deg)
DCP	1263	1263	1311	G	ν_{12} CH_2 wag	63.9	69	73
	1254	1253	1299	G	ν_{13} CH bend	57.4	50	58
	1234	1238	1268	T	ν_{13} CH bend	78.5	63	63
	667	685	660	T	ν_{21} C−Cl stretch	65.7	70	76
DCE	1234	1232	1264	T	ν_{9} CH_2 wag	75.3	73	76[b]
CP	1305	1304	1342	G	ν_{14} *CH_2 wag	57	54.7	77
	1263	1267	1292	T	ν_{14} *CH_2 wag	64.1	81	83[c]
	1257	1264	1290	G	ν_{15} CH_2 twist	66.6	70	70
	727	743	729	T	ν_{23} C−Cl stretch	61.7	71	81[c]
	650	664	647	G	ν_{23} C−Cl stretch	58.6	65	81

[a] The central C−C bond has been chosen as a common reference axis for the three chlorinated molecules and the corresponding ϕ angles with respect to the transition moment vectors are listed in the seventh column. α and α_{calc} are the angles between the transition moment vectors of the corresponding vibrational modes with respect to the *c* axis of the host crystalline phase, as experimentally evaluated by dichroism measurements and as evaluated by molecular modeling, respectively. [b] Weight-average between the α values calculated for the two minimum-energy locations of the T conformer of DCE ($\alpha_1 = 81°$, $\alpha_2 = 63°$; $E_2 - E_1 = 0.7$ kcal/mol). [c] Weight-average between the α values calculated for the two minimum-energy locations of the T conformer of CP (ν_{14}: ($\alpha_1 = 84°$, $\alpha_2 = 68°$); ν_{23}: ($\alpha_1 = 80°$, $\alpha_2 = 62°$); $E_2 - E_1 = 0.4$ kcal/mol).

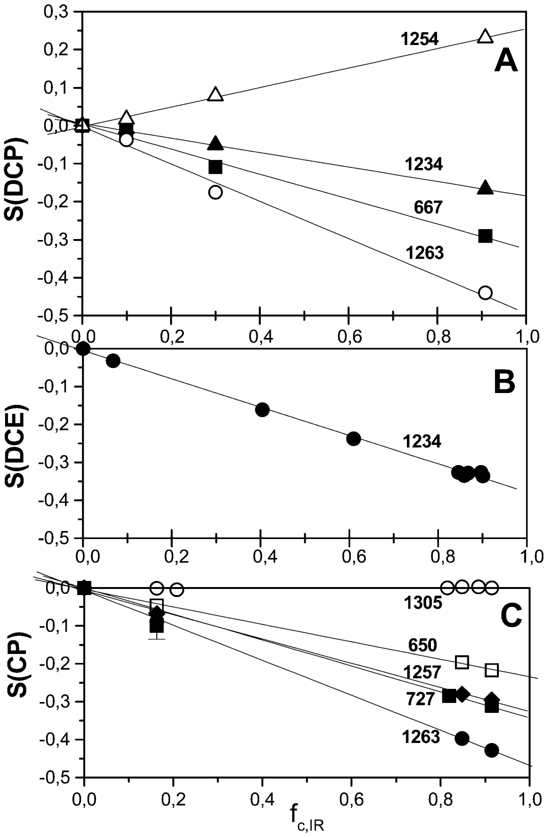

Figure 9. Infrared order parameter *S*, as evaluated by dichroic ratios of conformationally sensitive peaks of the three chlorinated guests, (A) DCP, (B) DCE, and (C) CP, vs the orientation factors relative to the helical chains of the host polymeric phase, as evaluated by the dichroic ratio of the 571 cm^{-1} infrared peak ($f_{c,IR}$). Empty and filled symbols correspond to gauche and trans conformers, respectively. The wavenumber of the peaks, as cm^{-1}, are reported close to the interpolation lines.

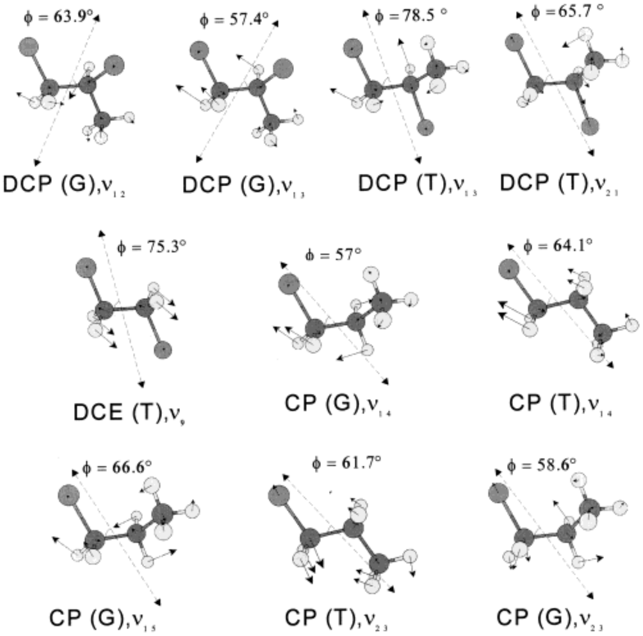

Figure 10. Vibrational modes and the transition moment vector directions with respect to the central C−C bond, calculated for the infrared peaks of Table 1, corresponding to T and G conformers of the three isolated chlorinated molecules.

peaks are obtained. Because of the availability of samples in a very broad range of crystalline phase orientation, the experimental error, mainly associated with the interpolation procedure, is generally smaller than ±3°.

Of course, only for the limiting case of a well-defined fixed location of the guest in the host lattice, these α values, experimentally evaluated for the different guest peaks, would correspond to the angles between their transition moment vectors and the chain axis of the polymeric host crystalline phase. For the opposite limiting case of complete guest mobility, in the time scale which characterizes FTIR spectroscopy (picoseconds), the guest peaks would be not dichroic. The application of eq 3 would result into an α value formally equal to the magic angle 54.7°.[14] As a consequence, for the case of partial guest mobility around a minimum-energy location, experimental procedures like that one of eq 3 and Figure 9 are expected to lead to α values which are shifted toward the magic angle (54.7°).

Transition Moment Directions of Vibrational Modes of Isolated Guest Molecules. Calculation of dipole moment derivatives with respect to the normal modes allows the evaluation of the vibrational transiton moment direction with respect to the molecular structure. For the sake of an easier comparison, the central C−C bond has been chosen as a common reference axis for the three chlorinated molecules, and the corresponding ϕ angles with respect to the transition moment vectors are listed in the seventh column of Table 1.

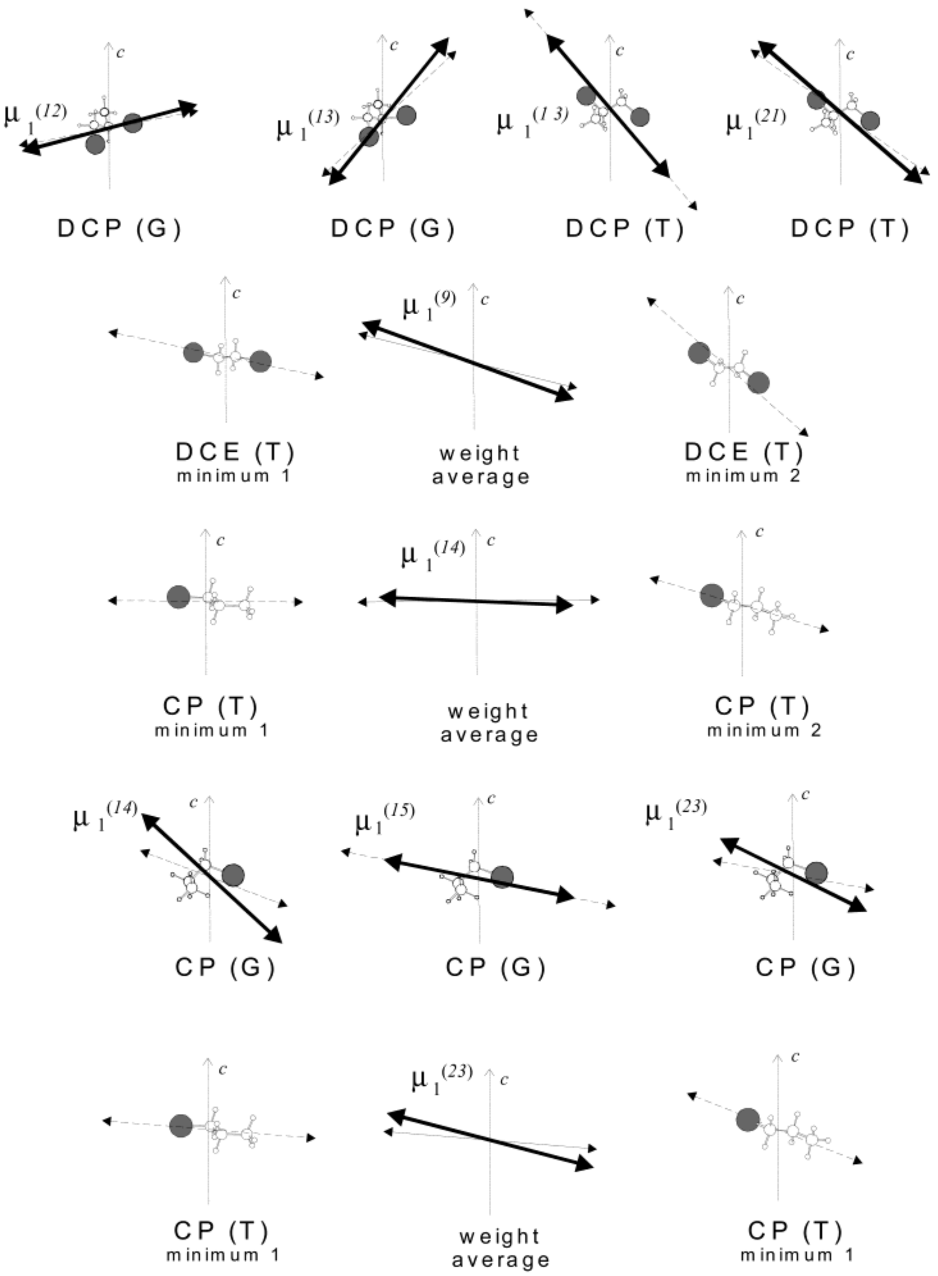

Figure 11. Energy minima orientations of the T and G conformers of the three chlorinated guest molecules with respect to the *c* axis of the host crystalline phase.[11] The transition moment vector directions, as calculated by molecular modeling and evaluated by infrared dichroism (corresponding to α_{calc} and α of Table 1), are shown as dashed and continuous arrows, respectively. As for the T conformers of DCE and CP, two minimum-energy orientations differing in energy of less than 1 kcal/mol are shown. Correspondingly, the experimentally evaluated transition moment vector direction has been compared with a Boltzmann-weighted average of the two calculated directions (central sketches of second, third, and fifth raw).

Moreover, the vibrational modes and the transition moment vector directions with respect to the central C−C bond, calculated for the considered infrared peaks, are shown by the models of Figure 10. It is worth noting that, for all the considered vibrational modes of the three chlorinated molecules, the transition moment directions correspond to ϕ angles in the relatively narrow range 57°−79°.

Molecular Modeling Calculation of Transition Moment Directions of Guest Vibrational Modes with Respect to the Chain Axis of the Host Crystalline Phase. Starting from the DFT calculated transition moment vectors, on the basis of the knowledge of the minimum-energy locations of the chlorinated guest conformers, evaluated in previous studies,[6,11] it is possible to calculate the angles between the transition moment vector and the chain axis of the host crystalline phase (α_{calc}, ninth column of Table 1).

In particular, the orientations of the guest conformers with respect to the *c* axis of the host crystalline phase, which correspond to the calculated energy minima for the guest molecules into the host cavity,[11] are sketched in Figure 11. As for the T conformers of DCE and CP, which present two minimum-energy locations differing in energy by less than 1 kcal/mol,[11] both corresponding orientations are sketched.

Comparison between Experimentally Evaluated and Calculated Transition Moment Vector Directions of Guest Vibrational Modes. A comparison between the directions of the transition moment vectors, as calculated by molecular modeling (dashed arrows, corresponding to α_{calc}) and experimentally evaluated by infrared dichroism (thick arrows, corresponding to α), is presented in Figure 11. As for the T conformers of DCE and CP, α_{calc} has been obtained as an average of the values calculated for both orientations, being weighted according to their relative calculated populations.

A first relevant result to be drawn by comparing the data of Table 1 and of Figure 11 is the good agreement between the α_{calc} and experimentally determined α angles for most peaks of the considered chlorinated guest molecules. This seems to confirm the validity of our experimental procedure to evaluate transition moment vector orientations of guest molecules as well as the molecular mechanics evaluations of the guest locations in the host cavities.

The average value of the difference between measured and calculated values of α ($\alpha_{calc} - \alpha$) for the considered chlorinated molecules is about 8°, which is close to the accepted accuracy of computational methods in evaluating vibrational transition moment directions (±10°).[23] It is however worth noting that, in our case, the calculated differences $\alpha_{calc} - \alpha$ result to be always positive. A possible origin of these regularly positive differences could be some guest mobility with respect to the host crystalline phase, in the time scale of the FTIR measurements (picoseconds).

The data of Table 1 indicate that large differences between calculated and measured α values have been observed only for the G conformer of CP, and particularly for the ν_{14} vibrational mode, whose absorption peak is not dichroic (see empty circles in Figure 9C), although a large value of α_{calc} has been calculated. A higher mobility of the CP guest seems reasonable since, between the considered guest molecules, it has the smallest molecular volume and the fastest desorption kinetics from the s-PS clathrate phase.[13]

Conclusions

Syndiotactic polystyrene films uniaxially stretched at different draw ratios, and including different crystalline (δ and γ) and clathrate phases (with DCP, DCE and CP), have been studied by combined infrared linear dichroism and X-ray diffraction measurements.

The axial orientation function of the host crystalline phase, as evaluated by X-ray diffraction measurements, is close to the maximum value for films drawn at draw ratios higher than 2.5, while it is substantially negligible for draw ratios lower than 1.5. Moreover, both the crystalline phase orientation and the dichroism of the polymer host peaks remain essentially unaltered as a consequence of guest absorption.

The chlorinated molecules, when guests of clathrate s-PS phases, present conformationally sensitive peaks which are generally highly dichroic, and their dichroism tends to increase with guest desorption, gradually reaching a plateau value, when the desorption from the amorphous phase has been completed. These high dichroic ratios clearly indicate that all the considered chlorinated molecules, independently of their conformation, when included as guests into the polymeric host lattice present some degree of order with respect to the draw direction.

The α angle between the crystallographic c axis (chain axis) and the transition moment vector of the vibrational mode for two polymeric host peaks, corresponding to long helical sequences (571 and 1320 cm^{-1}), has been evaluated by assuming orientation factors as evaluated by X-ray diffraction measurements. The knowledge of these α values allows an easy evaluation of the crystalline phase orientation for any helical s-PS sample, based simply on a dichroic ratio measurement for at least one of these two peaks.

For several conformationally sensitive guest peaks, the dichroic ratio and the order parameter S have been evaluated as a function of the draw ratio of clathrate s-PS films. By a quantitative comparison between dichroic ratios of helical polymer host peaks and of conformationally sensitive guest peaks, the directions of the transition moment vectors of several guest vibrational modes, with respect to the chain axis of the polymeric host lattice, have been evaluated.

Starting from DFT calculations of transition moment vectors of isolated guest molecules and on the basis of the knowledge of the minimum-energy locations of the chlorinated guest conformers, the directions of the transition moment vectors with respect to the chain axis of the polymeric host lattice have also been independently calculated.

The good agreement between calculated and experimentally determined moment vector directions for most vibrational modes of the considered chlorinated guest molecules validates our experimental procedure to evaluate transition moment vector orientations of guest molecules as well as of the molecular mechanics evaluations of the guest locations in the host cavities.

It is also suggested that the always positive differences between calculated and experimentally determined moment vector directions can be in principle used to get information relative to the guest mobility with respect to the host crystalline phase, on the time scale of the FTIR measurements (picoseconds). In this respect, the results of the present paper suggest that the mobility of the considered chlorinated guests is generally negligible, but for the case of the gauche conformer of 1-chloropropane.

Acknowledgment. Financial support of the “Ministero dell’Universita’ e della Ricerca Scientifica Tecnologica” (PRIN02 and Cluster26) and of Regione Campania (Legge 41 and Centro di Competenza) is gratefully acknowledged. We acknowledge the contributions to this work by Prof. Vincenzo Barone, Dr. Nadia Rega, and Dr. Giovanni Scalmani of the University of Naples, Dr. Vincenzo Venditto and Dr. Luciano Di Maio of the University of Salerno, and Dr. Riccardo Bianchi of Nuroll S.p.A.

References and Notes

(1) Ishihara, N.; Kuramoto, M.; Uoi, M. *Macromolecules* **1986**, *19*, 2035.
(2) Zambelli, A.; Longo, P.; Pellecchia, C.; Grassi, A. *Macromolecules* **1987**, *23*, 1539.
(3) Guerra, G.; Vitagliano, V. M.; De Rosa, C.; Petraccone, V.; Corradini, P. *Macromolecules* **1990**, *23*, 1539.
(4) Immirzi, A.; De Candia, F.; Iannelli, P.; Vittoria, V.; Zambelli, A. *Makrom. Chem., Rapid Commun.* **1988**, *9*, 761.
(5) Chatani, Y.; Shimane, Y.; Inoue, Y.; Inagaki, T.; Ishioka, T.; Ijitsu, T.; Yukinari, T. *Polymer* **1992**, *33*, 488.
(6) De Rosa, C.; Rizzo, P.; Ruiz de Ballesteros, O.; Petraccone, V.; Guerra, G. *Polymer* **1999**, *40*, 2103.
(7) De Rosa, C.; Guerra, G.; Petraccone, V.; Pirozzi, B. *Macromolecules* **1997**, *30*, 4147. (b) Milano, G.; Venditto, V.; Guerra, G.; Cavallo, L.; Ciambelli, P.; Sannino, D. *Chem. Mater.* **2001**, *13*, 1506.

(8) Guerra, G.; Manfredi, C.; Rapacciuolo, M.; Corradini, P.; Mensitieri, G.; Del Nobile, M. A. Ital. Pat. 1994 (C.N.R). (b) Reverchon, E.; Guerra, G.; Venditto, V. *J. Appl. Polym. Sci.* **1999**, *74*, 2077.

(9) Manfredi, C.; Del Nobile, M. A.; Mensitieri, G.; Guerra, G.; Rapacciuolo, M. *J. Polym. Sci., Polym. Sci. Phys. Ed.* **1997**, *35*, 133.

(10) Guerra, G.; Manfredi, C.; Musto, P.; Tavone, S. *Macromolecules* **1998**, *31*, 1329.

(11) Guerra, G.; Milano, G.; Venditto, V.; Musto, P.; De Rosa, C.; Cavallo, L. *Chem. Mater.* **2000**, *12*, 363. (b) Milano, G.; Guerra, G.; Cavallo, L. *Macromol. Theory Simul.* **2001**, *10*, 349.

(12) Guerra, G.; Venditto, V.; Mensitieri, G. It. Pat. SA00A23; Eur. Pat. Appl. EP1217360A2. (b) Mensitieri, G.; Venditto, V.; Guerra, G *Sens. Actuators* **2003**, *92*, 255.

(13) Musto, P.; Manzari, M.; Guerra, G *Macromolecules* **1999**, *32*, 2770. (b) Musto, P.; Manzari, M.; Guerra, G. *Macromolecules* **2000**, *33*, 143.

(14) Samuels, R. J. In *Structured Polymer Properties;* John Wiley & Sons: New York, 1971; Chapter 2, pp 28−37. (b) Kakudo, M.; Kasai, N. In *X-ray Diffraction by Polymers;* Elsevier: Amsterdam, 1972; Chapter 10, pp 252−259. (c) Read, B. E. In *Structure and Properties of Oriented Polymers*; Ward, I. M., Ed.; Appl. Sci. Publishers: London, 1975; Chapter 4, pp 150−184. (d) Jasse, B.; Koenig, J. L. *J. Macromol. Sci., Rev. Macromol. Chem.* **1979**, *C17*, 61.

(15) Alexander, L. E. In *X-ray Diffraction Methods in Polymer Science;* Robert E. Krieger: Huntington, NY, 1979; Chapter 4, pp 210−211. (b) Rizzo, P.; Lamberti, M.; Albunia, A. R.; de Ballesteros, O. R.; Guerra, G. *Macromolecules* **2002**, *35*, 5854. (c) Rizzo, P.; Albunia, A. R.; Milano, G.; Venditto, V.; Guerra, G.; Mensitieri, G.; Di Maio, L. *Macromol. Symp.* **2002**, *185*, 65.

(16) See e.g.: Califano, S. *Vibrational States;* John Wiley & Sons: London, 1976; pp 62−65.

(17) Gaussian 98: Frisch, M. J.; Trucks, G. W.; Schlegel, H. B.; Scuseria, G. E.; Robb, M. A.; Cheeseman, J. R.; Zakrzewski, V. G.; Montgomery, J. A., Jr.; Stratmann, R. E.; Burant, J. C.; Dapprich, S.; Millam, J. M.; Daniels, A. D.; Kudin, K. N.; Strain, M. C.; Farkas, O.; Tomasi, J.; Barone, V.; Cossi, M.; Cammi, R.; Mennucci, B.; Pomelli, C.; Adamo, C.; Clifford, S.; Ochterski, J.; Petersson, G. A.; Ayala, P. Y.; Cui, Q.; Morokuma, K.; Malick, D. K.; Rabuck, A. D.; Raghavachari, K.; Foresman, J. B.; Cioslowski, J.; Ortiz, J. V.; Stefanov, B. B.; Liu, G.; Liashenko, A.; Piskorz, P.; Komaromi, I.; Gomperts, R.; Martin, R. L.; Fox, D. J.; Keith, T.; Al-Laham, M. A.; Peng, C. Y.; Nanayakkara, A.; Gonzalez, C.; Challacombe, M.; Gill, P. M. W.; Johnson, B.; Chen, W.; Wong, M. W.; Andres, J. L.; Gonzalez, C.; Head-Gordon, M.; Replogle, E. S.; Pople, J. A. Gaussian, Inc., Pittsburgh, PA, 1998.

(18) Guerra, G.; Musto, P.; Karasz, F. E.; MacKnight, W. J. *Makromol. Chem.* **1990**, *191*, 2111. (b) Reynolds, N. M.; Hsu, S. L. *Macromolecules* **1990**, *23*, 3463.

(19) Tanabe, K. *Spectrochim. Acta* **1972**, *28A*, 407.

(20) Thorbjornsrud, J.; Ellestad, O. H.; Klaboe, P.; Torgrimsen, T. *J. Mol. Struct.* **1973**, *15*, 45. (b) Guirgis, G. A.; David Hsu, Y.; Charla Vlaservich, A.; Stidham, H. D.; Durig, J. R. *J. Mol. Struct.* **1996**, *378*, 83.

(21) Tanabe, K.; Saeki, S. *J. Mol. Struct.* **1975**, *27*, 79. (b) Ogawa, Y.; Imazeki, S.; Yamaguchi, H.; Matsuora, H.; Harada, I.; Shimanouchi, T. *Bull. Chem. Soc. Jpn.* **1978**, *51*, 748. (b) Durig, J. R.; Zhu, X.; Shen, S. *J. Mol. Struct.* **2001**, *570*, 1.

(22) Musto, P.; Tavone, S.; Guerra, G.; De Rosa, C. *J. Polym. Sci., Polym. Phys. Ed.* **1997**, *35*, 1055. (b) Musto, P.; Mensitieri, G.; Cotugno, S.; Guerra, G.; Venditto, V. *Macromolecules* **2002**, *35*, 2296.

(23) Radziszewski, J. G.; Downing, J. W.; Gudipati, M. S.; Balaji, V.; Thulstrup, E. W.; Michl, J. *J. Am. Chem. Soc.* **1996**, *118*, 10275.

MA034964X